

# American Journal of Science

MAY 1996

## THE NATURAL WEATHERING OF STAUROLITE: CRYSTAL-SURFACE TEXTURES, RELATIVE STABILITY, AND THE RATE-DETERMINING STEP

MICHAEL A. VELBEL, CHARLES L. BASSO, JR.\*,  
and MICHAEL J. ZIEG

Department of Geological Sciences,  
Michigan State University,  
East Lansing, Michigan 48824-1115

**ABSTRACT.** Mineral surface-textures on naturally weathered crystals of staurolite [monoclinic, pseudo-orthorhombic;  $\text{Fe}_4\text{Al}_{18}\text{Si}_8\text{O}_{46}(\text{OH})_2$ ] indicate that staurolite weathering is generally interface-limited. Etch pits on naturally weathered staurolites are disk-shaped, extensive parallel to (010), and thin perpendicular to (010). (010) is the plane of weak bonding and weak cleavage and the orientation of common stacking defects in the staurolite lattice, any of which could account for preferential dissolution in this orientation. Staurolite weathers very slowly relative to most other silicate minerals; this may be due to presence of stable kyanite-like "ribbons" in the staurolite structure or to the low site-energy of the Fe-site in the staurolite structure (compared to other orthosilicates). Staurolite weathering is interface-limited in most weathering environments. Although staurolite contains enough Al to coat itself completely with a non-porous protective surface layer of Al-hydroxides during weathering, protective surface layers apparently form only in some bauxites, where Al is abundant. The capacity of staurolite to form protective surface layers around itself in most weathering environments is apparently limited by its slow weathering, which prevents the release of product-forming elements (especially Al) at rates sufficient to produce local supersaturation with respect to secondary minerals.

### INTRODUCTION

The purpose of this study is to characterize the crystallographic control of the natural weathering of staurolite and to determine the rate-determining mechanism of the staurolite weathering reaction from the surface textures of naturally weathered staurolite.

Staurolite is an orthosilicate. The natural weathering of other common orthosilicates (olivine, garnet) is well studied (Velbel, 1993). However, there is only one published experimental study of staurolite dissolution (Nickel, 1973), and there are few published reports of the alteration textures of naturally weathered staurolite; to our knowledge, none involves examination of surface textures with scanning electron micros-

\* Present address: Department of Geology, University of Toledo, Toledo, Ohio 43606.

copy. Thus, study of staurolite weathering broadens the range of crystal-chemical varieties of orthosilicates that have been investigated and adds to our understanding of the influence of crystal-chemical factors on the kinetics of silicate mineral-water interactions.

*Previous work.*—Mineral-surface textures give insight into the rate-determining step in mineral-water interactions. Any mineral-water interaction (for example, hydrolysis of silicate minerals during rock weathering) requires a sequence of steps for the reaction to proceed. If all reactants are available in excess, the following steps must occur (in sequence): (1) aqueous reactants must arrive at the mineral-solution interface; (2) the reaction must occur at the interface; and (3) dissolved products must leave the site of the interfacial reaction (lest they accumulate to the extent that equilibrium is attained or the reaction is otherwise suppressed). When a number of different reaction steps occurs in series, the slowest step is rate-determining. Therefore, one of two mechanisms is rate-determining in the weathering of silicate minerals: (1) transport control (or transport-limited reaction), in which transport of aqueous reactants to or products from the fresh mineral surface is the slow (rate-determining) step in the reaction; or (2) surface-reaction (interface) control (or interface-limited reaction), in which the rate of the reaction is determined by processes occurring at the mineral-solution interface (Berner, 1978, 1981).

Each rate-determining mechanism has unique consequences for the microscopic surface morphology of weathered mineral grains (Berner, 1978, 1981). Diffusion is the slowest form of transport (Berner, 1978, 1981); in the case of silicate-mineral weathering, the only medium through which diffusion could be slow enough to be rate limiting is a protective surface-layer of residual or secondary solids on the surface of the dissolving mineral (Berner, 1978, 1981; armoring precipitate *sensu* Schott and Petit, 1987). Surfaces of reactant minerals weathering by transport control are smooth, rounded, and featureless, reflecting the uniformity of attack on the surface (Berner, 1978, 1981), and protective surface layers of secondary products are observed on certain minerals in association with such surfaces (Velbel, 1984, 1993). Interface-limited mechanisms produce etch pits and related features, reflecting the site-selective nature of the interfacial reaction (Berner, 1978, 1981).

Velbel (1993) reviewed the distribution of these surface textures on naturally weathered silicate minerals. Etch pits are ubiquitous on major rock-forming silicates (feldspar, pyroxene, amphibole, olivine, quartz), whereas either etch pits or protective surface layers can occur on almandine and spessartine garnet, depending on local geochemical conditions in the weathering microenvironment (Velbel, 1993).

Staurolite [ideally,  $\text{Fe}_4\text{Al}_8\text{Si}_8\text{O}_{46}(\text{OH})_2$ ; Hawthorne and others, 1993c] is an orthosilicate (nesosilicate). Members of the orthosilicate group include both the most easily weathered and the most resistant silicate minerals (olivine and zircon, respectively; Morton, 1984, 1985; Bateman and Catt, 1985). This observed large range of susceptibilities to weather-

ing cannot be a consequence of different degrees of silica polymerization, as all orthosilicates contain completely unpolymerized silica tetrahedra. Therefore, the differential susceptibility of different orthosilicates to weathering must involve differences in the crystal chemistry of sites other than the silica tetrahedral sites. Also, orthosilicates include examples of silicate minerals on which etch pits and interface-limited weathering reactions are ubiquitous (olivine) and examples in which the formation of diffusion-limiting protective surface layers is widespread (almandine and spessartine garnets) (Velbel, 1993, and references therein). Velbel (1993) predicted that staurolite would produce protective surface layers under weathering conditions in which Al behaves conservatively and forms high-molar-volume secondary trihydroxides (as opposed to lower-molar-volume oxyhydroxides or sesquioxides).

Most of what is known about the alteration of staurolite is known from studies of heavy-mineral stability in the sedimentary cycle. Much of this literature is based on studies of relative mineral abundances, and how these abundances are modified by weathering (see reviews by Bateman and Catt, 1985, and Morton, 1984, 1985) and burial diagenesis (post-depositional heavy-mineral dissolution in clastic sedimentary strata [intrastratal dissolution]; Morton, 1984, 1985). A portion of this literature also reports the surface textures of altered heavy minerals. Morton (1979, 1984) presents scanning electron microscope images of etched staurolite, although all his examples are from burial diagenetic environments. Several studies of laterite and bauxite genesis on staurolite-bearing parent rocks (van Kersen, 1955; Edou-Minko, 1988) briefly discuss staurolite alteration textures relevant to this paper; these observations are discussed below.

#### MATERIALS AND METHODS

##### Samples

Staurolite crystals from six localities in North and South America were examined for this study. The six sampling localities are listed and discussed in approximate order of increasing degree of weathering of the matrix surrounding the staurolite (table 1).

TABLE 1  
*Sample locality and analytical summary*

Locality	# of grains (SEM)	# of thin sections
Fernleigh, Ontario, Canada	2	5
Imperial Heights, Michigan	6	0
Coweeta, North Carolina	109	4
Blue Ridge, Fannin County, Georgia	7	0
Ball Ground, Cherokee County, Georgia	2	0
Moengo Hill, Suriname	0	2

*Fernleigh, Ontario (Canada).*—Staurolite occurs in a large glacially sculpted outcrop of the Flinton Group (Grenville Supergroup) near Fernleigh (Hounslow and Moore, 1967; Carmichael, Moore, and Skippen, 1978). Disaggregation of the enclosing schistose matrix caused euhedral kyanite and garnet crystals to accumulate in depressions on the outcrop surface. Staurolite crystals were exhumed from their better-indurated schistose matrix only with difficulty. Two large ( $> 1$  cm) crystal fragments were examined by SEM; five thin sections from the MSU petrology teaching collection were examined by petrographic microscope.

*Imperial Heights, Michigan (USA).*—Staurolite occurs in small outcrops of the Michigamme Slate (Precambrian) in the western Upper Peninsula of Michigan. Most of the Michigamme Slate was metamorphosed to greenschist facies, but several locations of amphibolite facies are known (James, 1955). At the locality sampled for this study (Cambray, 1977), a band of staurolite schist occurs in a glacially rounded knob of amphibolite facies Michigamme Slate that has been exposed to weathering since deglaciation. Destruction of the schistose matrix (by some combination of weathering of individual minerals and intergranular disintegration) around the 5 to 10 mm staurolite crystals has left the more resistant staurolite crystals standing in relief above the less-resistant matrix. Numerous staurolite crystals were exhumed completely from the surrounding matrix and were washed into patches of moss in depressions within and around the outcrop, from which matrix-free individual crystals were easily recovered. Six large (5-10 mm) crystals were examined by SEM.

*Coweeta, North Carolina (USA).*—Staurolite occurs in the Tallulah Falls Formation (Precambrian-Lower Paleozoic), an amphibolite-facies metasedimentary unit of the southern Blue Ridge Mountains (Hatcher, 1979, 1980, 1988). The sampling locality for this study is in the Coweeta Hydrologic Laboratory of the U.S. Department of Agriculture, Forest Service, near Franklin, North Carolina. Much of the metamorphic rock in this area has been transformed to saprolite to depths up to 20 m, but the staurolite-rich intervals are somewhat more resistant to weathering. Consequently, staurolite occurs not as resistant mineral grains in a decayed saprolitic matrix but in layers of relatively well-indurated rock. These samples were suitable for thin-sectioning, but required crushing to liberate millimeter-scale staurolite crystals for SEM examination. One hundred and nine sand-size ( $\pm 1$  mm) grains were examined by SEM, and four standard-size thin sections were examined by petrographic microscope.

*Blue Ridge and Ball Ground, Georgia (USA).*—Georgia contains several of the famous staurolite-producing areas in North America. We examined staurolites from two localities: Blue Ridge (southern Fannin County) and Ball Ground (northern Cherokee County). At both sampling localities, schistose matrix derived from the weathering of the Bill Arp Formation (Proterozoic-Lower Paleozoic; M. W. Higgins, personal communica-

tion) has weathered to saprolite, leaving centimeter-scale staurolite crystals that were recovered by simply washing the sample. Seven large (1 cm) crystals from Blue Ridge (Fannin County) and two from Ball Ground (Cherokee County) were examined by SEM.

*Moengo Hill, Suriname (South America).*—Staurolite schist of the Orapu and Balling Formations (Precambrian) has weathered to bauxite in the vicinity of Moengo, Suriname (van Kersen, 1955). Two oversize thin sections were cut from a single hand-specimen of a ferruginous, pseudo-brecciated concretionary bauxite. Only petrographic observations were possible for this sample; it was not possible to liberate individual staurolite crystals from the well-indurated bauxite.

### Methods

Optical petrography and scanning electron microscopy (SEM) were used to examine naturally weathered staurolites. Whole-rock specimens suitable for thin-sectioning were available from only three of the study localities (table 1); 11 thin sections were prepared and examined with a Leitz Ortholux II-pol petrographic microscope. More than 100 individual staurolite crystals (representing 5 localities) were examined by SEM (table 1). Large (centimeter-scale) staurolite crystals were collected individually in the field or separated manually from weathered matrix material in the laboratory. Weathered rock samples containing small (millimeter-scale) staurolite crystals were crushed, and staurolite crystals with recognizable crystal faces or cleavage surfaces were individually picked from the debris with the aid of a binocular microscope. Small crystals were properly oriented for SEM mounting by agitating a quantity of grains in a small tray and allowing the individual grains to come to rest upon their largest flat surface (that is, crystal face or cleavage surface). Staurolite crystals were mounted to SEM stubs with double-sided adhesive tape, and a conductive gold coating was applied by sputtering. Specimens were examined using a JEOL JSM T-20 SEM.

Euhedral staurolite crystals (untwinned) were used for SEM examination. The relationship of preferentially oriented surface features (for example, etch pits) to the crystallography of the parent mineral could be ascertained from their relationship to zone axes determined from intersecting faces. Staurolite is monoclinic-prismatic ( $C2/m$ ) at room temperature but is pseudo-orthorhombic ( $90.00 \leq \beta \leq 90.45^\circ$ ; Hawthorne and others, 1993a,b). It was long believed that staurolite is orthorhombic (Donnay and Donnay, 1983; Hawthorne and others, 1993b). For simplicity, traditional (orthorhombic) nomenclature for faces and forms is used here, and the morphological (rather than X-ray structural) axial ratio is used ( $a:b:c_{\text{morph}} = 0.471:1:0.680$ ;  $a:b:c_{\text{struc}} = 0.471:1:0.340$ ; Donnay and Donnay, 1983). Figure 1 shows an idealized staurolite crystal and the nomenclature of the forms: the prism  $m\{100\}$ , the side  $b\{010\}$  and basal  $c\{001\}$  pinacoids, and the pinacoid (parallelohedron)  $r\{101\}$ . In the case of true orthorhombic symmetry (long assumed to hold for all staurolite; Donnay and Donnay, 1983),  $\{101\}$  is a rhombic prism; hence the tradi-

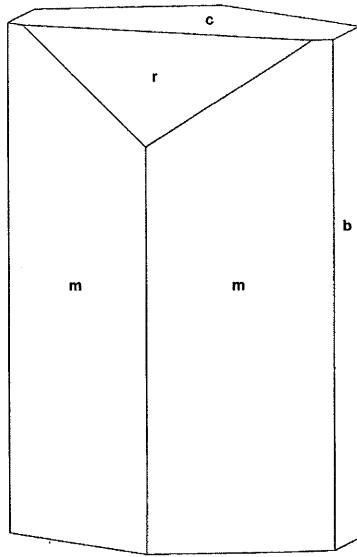


Fig. 1. Idealized staurolite crystal, showing nomenclature of crystal forms used in this study; prism  $m\{110\}$ ; side  $b\{010\}$  and basal  $c\{001\}$  pinacoids; and pinacoid (parallelohedron)  $r\{101\}$ . Crystal drawing generated using computer program SHAPE (Dowty, 1988).

tional designation  $r$ . All crystals used in this study that show faces in the form  $r\{101\}$  are from the Blue Ridge (Fannin County) Georgia sampling locality, and most are morphologically monoclinic, consistent with the findings of Donnay and Donnay (1983) and Hawthorne and others (1993b).

#### Observations

*Scanning electron microscopy.*—Samples from the Fernleigh, Ontario, outcrop (the least-weathered outcrop sampled for this study) exhibited only exposed poikiloblastic inclusions (for example, quartz, mica) at the staurolite surface and compromise surfaces with surrounding grains (that is, "impressions" of the surrounding schist), both textures similar to those reported by Gupta and Guha (1985). Staurolite in the Ontario samples is unweathered and will not be discussed further.

SEM examination revealed etch pits on naturally weathered staurolites from the other four localities examined by this technique. Etch pit distribution, orientation, and shape are all very similar from one sample to the another. There are differences in etch-pit size and depth from one grain to another. These variations are visible even among different crystals from the same sampling localities.

Etch pits on faces in the form  $m\{110\}$  occur initially as shallow lenticular depressions (fig. 2) elongate parallel to the  $z$ -axis (figs. 2-4). As they grow, etch pits deepen parallel to  $(010)$  (fig. 5). Features with similar

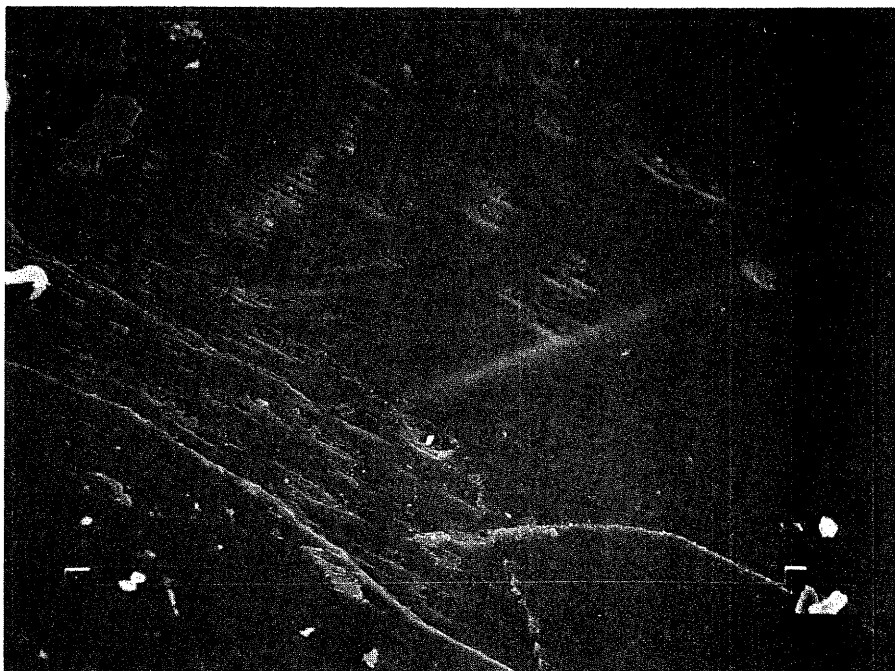


Fig. 2. Shallow lenticular depressions on  $m\{110\}$  elongate parallel to the  $z$ -axis (upper left to lower right). Sample C80-7-13A II-1, Coweeta, North Carolina. Scale marks are 100 microns apart.

shapes and orientations are observed on  $r\{101\}$  (figs. 6, 7). On faces of the  $b\{010\}$  pinacoid, etch pits occur as shallow lenticular depressions (fig. 8, 9). Deep etch pits on  $m\{110\}$  and  $r\{101\}$  and the shallow lenticular pits on  $b\{010\}$  have a flat, inequant disk-like morphology, the plane of the disk being the  $x$ - $z$  (010) plane; their long dimensions parallel [001], intermediate dimensions parallel [100], and the short dimensions parallel [010]. Thus, the preferential directions of dissolution and etch pit growth are along (010); etching is much slower perpendicular to this plane.

Etch pits occur primarily on bare staurolite surfaces but also occur beneath and between thin, discontinuous, porous, cracked patches of weathering products (fig. 10).

One grain from Coweeta, North Carolina, possesses a thick, continuous layer of well-crystallized euhedral material (fig. 11); the staurolite surface beneath this layer is devoid of etch pits (fig. 12). However, this material is probably not a weathering product. Compositional data are not available, and there is insufficient material for powder X-ray diffraction, but the alteration products have the morphology of corundum and/or hematite (hexagonal-trigonal; rhombohedron truncated by  $c$ -



Fig. 3. Larger, more numerous etch pits on  $m\{110\}$  elongate parallel to the  $z$ -axis (approx left to right). Sample IH-1, Imperial Heights, Michigan. Scale marks are 1 mm apart.

pinacoid; fig. 11). This isolated example is likely a high-temperature mineral assemblage and alteration texture; neither hematite with this habit nor corundum are common products of weathering or other low-temperature alteration (Deer, Howie, and Zussman, 1962, 1992; Welton, 1984). It will not be discussed further here.

*Optical petrography.*—On most silicate minerals, etch pits and replacement textures, although best seen with the SEM, are commonly visible petrographically (Velbel, 1993). Under the petrographic microscope, staurolite exhibits essentially no signs of weathering, indicating that etch pits or other surface features must be small, if present; this is consistent with the SEM results (figs. 2-12). Staurolites from the Ontario and North Carolina localities are not visibly altered in petrographic thin section. In the Ontario samples, no other silicates are weathered, either. In contrast, other iron-bearing silicates are visibly weathered in thin sections from the North Carolina samples. Here, typical centripetal replacement textures of limonite after garnet are common on almandine garnet in the same thin sections (Velbel, 1984, 1993). This is the case even where the garnet and the staurolite have experienced identical weathering histories (for



Fig. 4. Higher magnification image of same face as in figure 3. Sample IH-1, Imperial Heights, Michigan. Scale marks are 100 microns apart (compare with fig. 2). The right scale marker is directly above the first and second zero in "1000" and is partially obscured by the small bright particle there.

example, the two minerals are immediately adjacent to or even in contact with one another in thin section). Similarly, biotite and chlorite in the same thin sections are visibly oxide-stained. In North Carolina samples where all four of these Fe-bearing metamorphic silicates coexist, staurolite is commonly the only one that does not exhibit weathering features visible with optical techniques.

Staurolite and quartz are the only primary metamorphic minerals to survive weathering in the bauxites from Suriname. No modification of euhedral staurolite was observed, other than the introduction of thin ferruginous veins along transmineral fractures. These veins are visibly identical with the bauxite matrix, from which they are presumably derived. Alveoporumorphic replacements (terminology of Delvigne, ms) of limonite after almandine (representing complete destruction of almandine and replacement by limonite along grain boundaries and transmineral fractures) are widespread, even where the parent garnet was poikilitically included within the staurolite. Where schistose rock fragments served as the cores of bauxitic concretions, all primary minerals, including micas, feldspars, and garnets, have been completely destroyed. In



Fig. 5. Etch pits elongate parallel to z-axis (approx left to right) but much deeper parallel to (010) than in previous examples. Sample IH-2, Imperial Heights, Michigan. Scale marks are 100 microns apart (compare with figures 2 and 4).

contrast, staurolite in the same sample survives as discrete euhedral crystals and intact fragments reoriented relative to one another during bauxite formation.

#### DISCUSSION

*Crystallographic and crystal-chemical control of staurolite etching.*—Etch pits on naturally weathered staurolites are disk-shaped, extensive parallel to (010), and thin perpendicular to (010). Staurolite grains subjected to intrastatal dissolution in sandstones are much more extensively etched, and their etching exhibits the same preferred orientation (Morton, 1979, 1984).

The staurolite structure is traditionally described as slabs of kyanite  $[\text{Al}_2\text{SiO}_5]$  interleaved with Fe-Al oxide-hydroxide monolayers alternating along [010] (Hawthorne and others, 1993a). The kyanite slabs are not pure; there is minor but significant and ubiquitous substitution of Al for Si in tetrahedral sites and of Mg and Fe for Al in octahedral sites (Hawthorne and others, 1993a).

Alternating along [010] with the kyanite layers are vacancy-rich Fe-Al oxide-hydroxide monolayers [approx  $[\text{VI}]\text{Al}_{0.7}[\text{IV}]\text{Fe}_2\text{O}_2(\text{OH})_2$ ] (Hawthorne and others, 1993a). Most Fe in staurolite is divalent and occupies

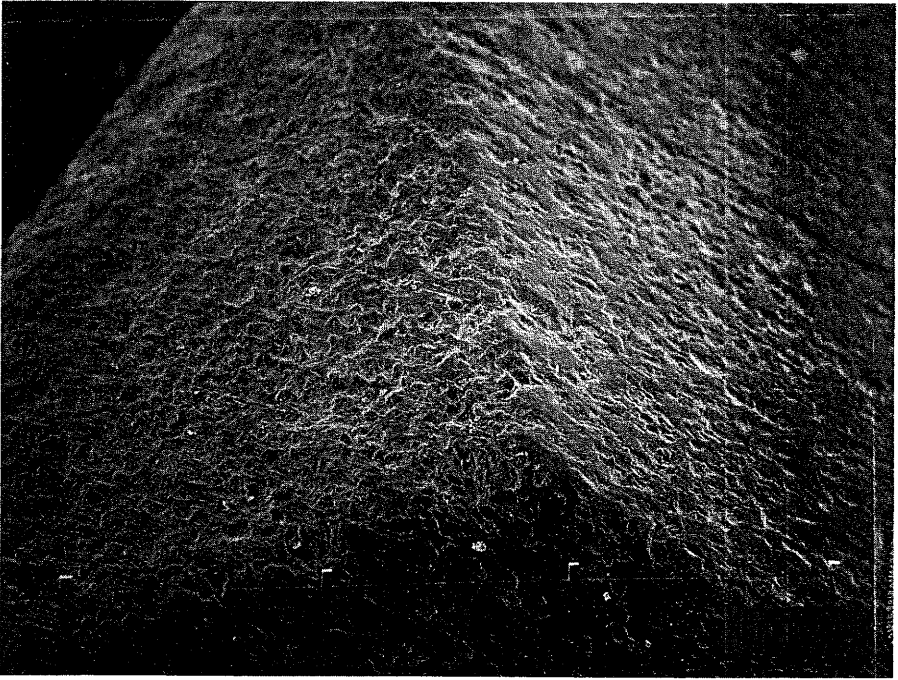


Fig. 6. Low-magnification image of  $m[110]$  (right) and  $r[101]$  (left); compare with figure 1 (z-axis is oriented from upper left to lower right). Sample R5, Blue Ridge, Fannin County, Georgia. Scale marks are 1 mm apart.

tetrahedral sites (Hawthorne and others, 1993a, p. 578; Deer, Howie, and Zussman, 1992); less than ten percent of Fe is trivalent (Dyar and others, 1991; Holdaway and others, 1991; Deer, Howie, and Zussman, 1992). According to some references (Berry and others, 1983; Deer, Howie, and Zussman, 1992; Blackburn and Dennen, 1994), staurolite exhibits (010) cleavage. Cation sites in the Fe-Al monolayer are only partially occupied, and weak metal-OH bonds are concentrated there; this weak bonding has been invoked to explain the (010) cleavage (Griffen and Ribbe, 1973; Ribbe, 1982). Weak bonding in this part of the crystal structure may also explain the preferred directions of dissolution implied by the orientation and geometry of the etch pits observed in this study. Etch pits are long and deep parallel to the (010) and narrow perpendicular to (010), parallel to the orientation of both the kyanite-like slabs, and the Fe-Al oxide-hydroxide monolayers between them.

Extended defects (stacking faults) have also been observed along (010) in staurolite (Lefebvre, 1982; Ribbe, 1982). Etch pits are known to nucleate on surface sites of excess energy, including twin boundaries and intersections of dislocations with crystal surfaces (Berner, 1978, 1981).

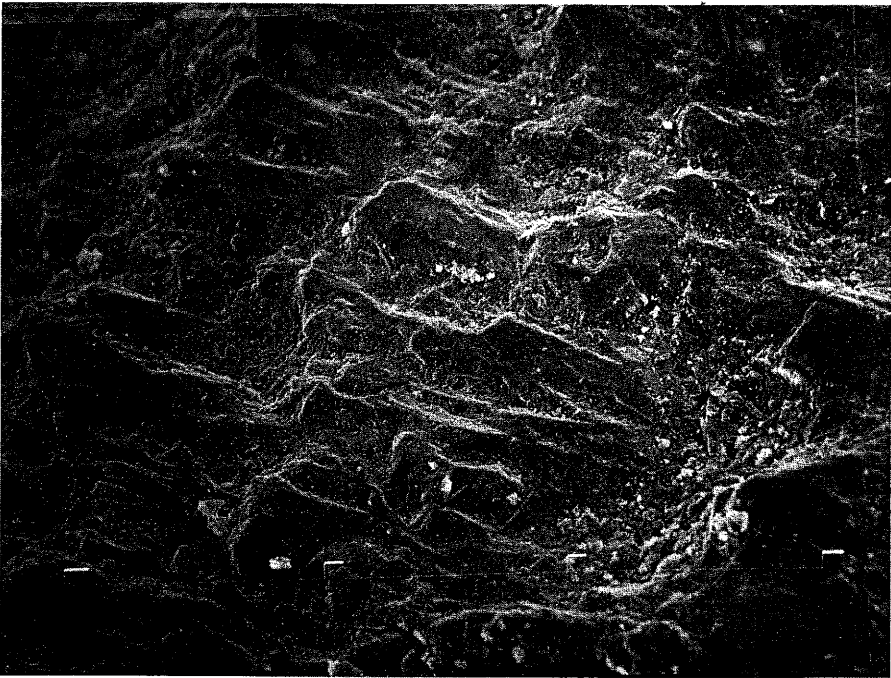


Fig. 7. Higher magnification image of  $r\{101\}$  face from figure 6. Sample R5, Blue Ridge, Fannin County, Georgia. Scale marks are 100 microns apart (compare with figs. 3 and 4).

Consequently, extended defects along (010) may also account for the orientation of etch pits on staurolite.

*Evidence for interface-limited weathering of staurolite.*—The near-ubiquity of etch pits on the faces of naturally weathered staurolite crystals examined for this study indicates that staurolite weathering is generally interface-limited. The thin, discontinuous, porous, cracked weathering products locally associated with the etch pits do not retard solute transport to or from the reactant-mineral surface.

*Evidence for formation of protective surface layers and transport-limited weathering of staurolite.*—Textures suggestive of protective surface layers and diffusion-limited kinetics were not observed in this study. Similarly, staurolite exhibits no replacement textures in bauxite from Onverdacht, Suriname (van Kersen, 1955, fig. 64). However, possible replacement textures resembling protective surface layers were reported by van Kersen (1955) on other samples of bauxite from Moengo Hill, Suriname. Van Kersen's (1955) figures 60 and 61 (and text referring thereto, p. 326) show partial alteration of staurolite to gibbsite in both transmitted and reflected light microscopy. His figure 61 clearly shows replacement; the



Fig. 8. Etch pits on  $m\{110\}$  (lower two-thirds of image; figure 5 is a high-magnification view of this same face) and  $b\{010\}$  (upper one-third of image). Etch pits occur as shallow lenticular depressions on  $b\{010\}$ . Sample IH-2, Imperial Heights, Michigan. Scale marks are 100 microns apart.

textures in his figure 60 could be either thin zones of peripheral replacement or gibbsite precipitates coating a passive (unweathered) staurolite substrate. Direct replacement of staurolite by gibbsite has also been reported by Edou-Minko (1988) from a study of lateritic profiles near Ouala, Gabon. However, textural observations are inconclusive because of the generally rough, anhedral character of the parent staurolite at this locality (Edou-Minko, 1988). Apparently, if protective surface layers of weathering products form on staurolite at all, they do so only in some bauxitic and lateritic weathering profiles.

*Staurolite weathering relative to other silicate minerals.*—Staurolite apparently weathers very slowly compared with other rock-forming silicate minerals in all weathering environments examined for this study. This is attested to by numerous observations in the field as well as in the laboratory: (1) Staurolite crystals stand in raised relief above weathered matrix at the Imperial Heights, Michigan, sample locality. (2) Staurolite crystals are easily exhumed from weathered saprolitic matrix at the Blue Ridge and Ball Ground, Georgia, sample localities. Both these observations imply that staurolite weathers more slowly than the schistose

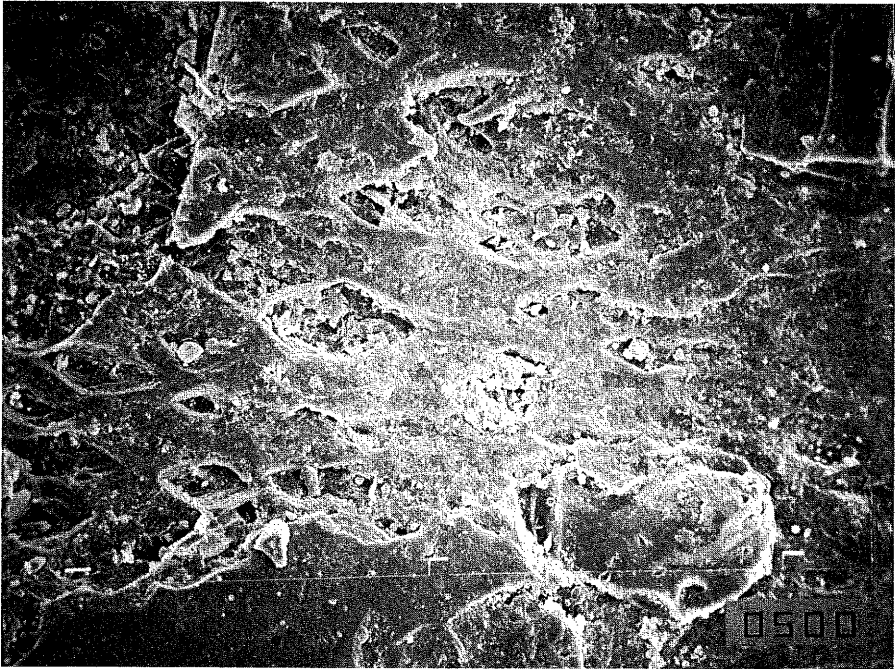


Fig. 9. Broad, shallow etch pits, elongate parallel to z-axis (approx left to right), on  $b\{010\}$ . Sample IH-2 (different orientation than fig. 8), Imperial Heights, Michigan. Scale marks are 100 microns apart.

matrix. (3) Staurolites at the Coweeta, North Carolina, sample site are not visibly altered in petrographic thin section. In samples where almandine, biotite, chlorite, and staurolite coexist, staurolite is commonly the only mineral not visibly weathered. (4) Staurolite and quartz are the only primary metamorphic minerals to survive weathering at Moengo Hill, Suriname. As at Coweeta, North Carolina, other silicate minerals in the bauxite from Suriname are preferentially weathered; however, unlike the case at Coweeta, the other Fe-silicates are completely destroyed under the more extensive weathering represented by the profile at Moengo Hill, Suriname. Staurolite survives here as discrete euhedral crystals in bauxite, as reoriented but otherwise unaltered fragments in bauxite, and as a heavy mineral in sediments derived from the bauxitic weathering profile (van Kersen, 1955).

Staurolite weathering rates are trivially slow compared with all other silicate minerals except quartz, at all localities sampled for this study. This is consistent with the results of previous studies of heavy-mineral weathering (see reviews by Morton, 1984, 1985, and Bateman and Catt, 1985), in which zircon, tourmaline, and minerals of the  $Al_2SiO_5$  group are the

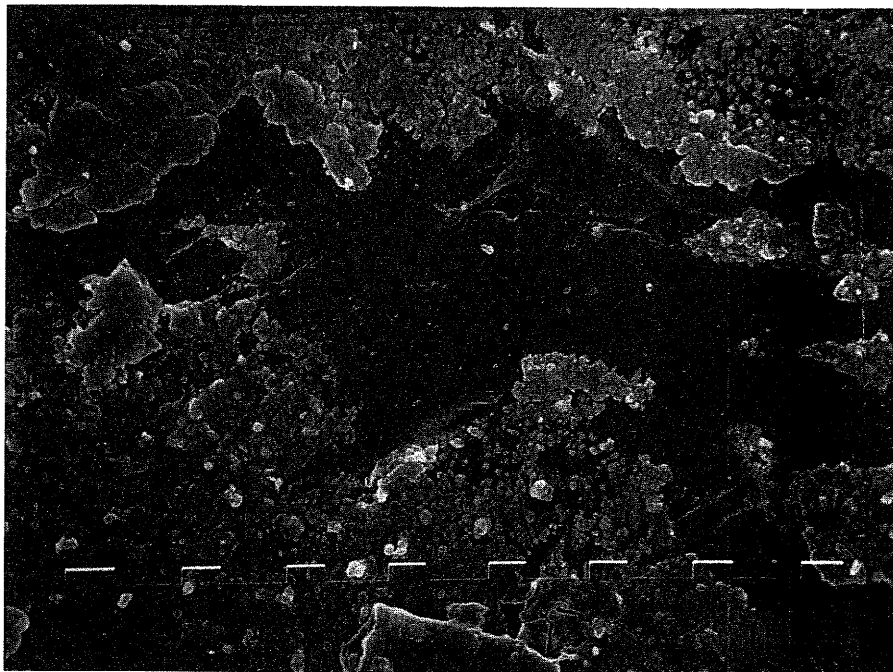


Fig. 10. Etch pits beneath and between thin, discontinuous, porous, cracked patches of weathering products. Sample ABT18C III-2, Coweeta, North Carolina. Scale marks are 100 microns apart.

only silicate minerals more resistant to weathering than staurolite. In the lateritic weathering profiles of Ovale, Gabon, staurolite abundance decreases up-profile, but it is generally almost as resistant as tourmaline, kyanite, and quartz (Edou-Minko, 1988). Slow weathering of staurolite relative to other silicate minerals is also broadly consistent with the experimental dissolution rates determined by Nickel (1973).

Dissolution and etching are evident from all weathered staurolite grains examined with SEM. However, the scale and extent of staurolite etching during weathering are modest compared with the etching of other silicate minerals, which can often be clearly seen in thin section or grain-mount, and which is commonly dramatic under SEM (Velbel, 1993). The reported absence of etch features on staurolites from podzolic soil profiles of temperate climates (Bateman and Catt, 1985) is most likely not real but methodological. Most soil heavy-mineral studies use optical microscopy; the present study indicates that etch pits on staurolite can only be observed by SEM. Thus, using optical petrography to classify grain morphology, either alone or to "screen" grain surface textures for later SEM study, would result in staurolite being classified as unetched and unweathered.



Fig. 11. Thick, continuous layer of alteration product (probably corundum  $\pm$  hematite) along fracture in staurolite from Coweeta, North Carolina (sample ABT 18C III-3). Scale marks are 10 microns apart.

Slow weathering of staurolite relative to other silicate minerals may be related to stability of kyanite-like "ribbons" parallel to (010) (which is also the elongation direction of the etch pits) in the staurolite structure. Kyanite and staurolite have essentially identical stability in the weathering environment, according to empirical mineral weathering series (Morton, 1984, 1985; Bateman and Catt, 1985). Another factor that may contribute to the slow rate of staurolite weathering relative to other Fe-bearing orthosilicates (garnet, olivine) involves the coordination of Fe in the structure. Coordination number is related to cation radius (and, consequently, bond length); smaller cations have smaller coordination numbers and shorter bond lengths with coordinating anions. Weathering rates of structurally related alkaline-earth orthosilicates are proportional to the radius of the cation (Casey and Westrich, 1992; Westrich and others, 1993). Iron occurs in tetrahedral sites in staurolite, octahedral sites in olivine, and distorted cubic sites in garnet; as coordination number increases, so does the bond length (Smyth and Bish, 1988). Longer bonds between the same two ions are weaker than shorter bonds (the site energy for the Fe site in staurolite is lower than the site-energies

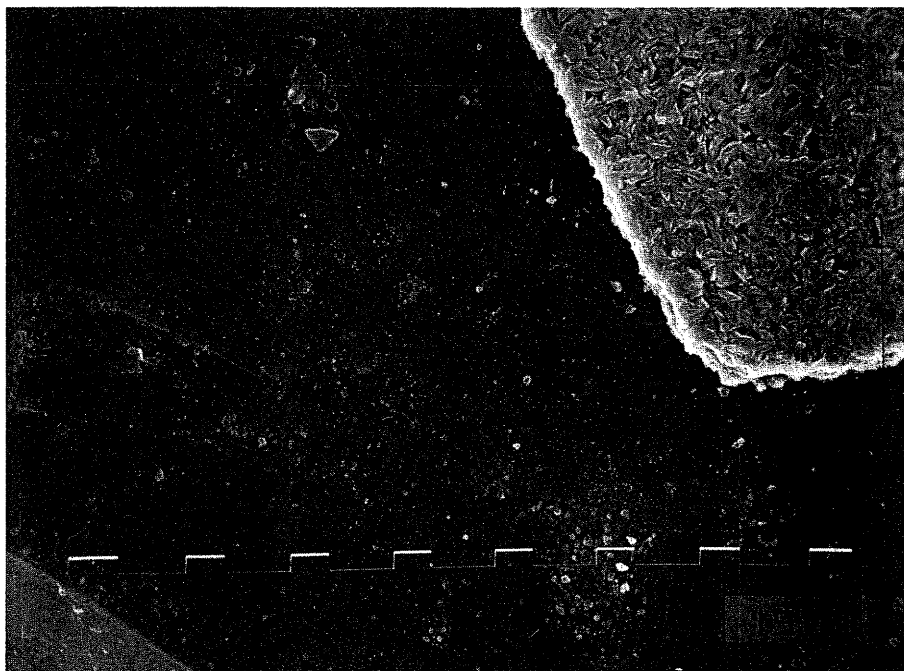


Fig. 12. Staurolite surface beneath regions from which layer shown in figure 11 was removed during sample preparation. The surface beneath the layer is devoid of etch pits. Sample ABT 18C III-3, Coweeta, North Carolina. Scale marks are 10 microns apart.

for Fe sites in garnet and olivine [Smyth and Bish, 1988]; in general, silicate dissolution rates vary with site energy, Brady and Walther, 1992); thus, disruption of individual Fe-O bonds may be easier in garnet and olivine than in staurolite. Either or both of these two reasons could explain why staurolite weathers so much more slowly than other silicates under similar conditions. Differences in the valence state of the Fe are not responsible; as noted above, Fe in staurolite is predominantly divalent (Hawthorne and others, 1993a; Dyar and others, 1991; Holdaway and others, 1991), as in garnet and olivine.

#### SUMMARY AND CONCLUSIONS

Elongate etch-pits form during the initial natural weathering of staurolite, penetrating the grain surface parallel to incipient cleavages, common defects, and/or planes of weak bonding, all of which parallel (010) in the staurolite lattice. Etching continues by elongation and deepening of these etch pits parallel to (010), with little or no change in width. The near-ubiquity of etch pits observed by SEM favors the hypothesis that the kinetics of staurolite weathering are generally interface-limited rather than transport-limited.

Minerals that have the potential to form protective surface layers (for example, near-endmember almandine and spessartine garnet; staurolite) can do so only if the major cations constituting the secondary minerals (for example, Al) behave conservatively (Velbel, 1993). If geochemical conditions in the weathering microenvironment permit mobilization of these elements, protective surface layers cannot form, and interface-limited kinetics prevail (Velbel, 1993). This is observed in some instances of the weathering of almandine garnet (Velbel, 1984, 1993). Thus, the widespread occurrence of etch pits on naturally weathered staurolites suggests that Al is mobilized (removed from the dissolution site) and behaves non-conservatively during staurolite weathering, at least at the scale of the etch pits. The capacity of staurolite to form protective surface layers around itself in most weathering environments is apparently limited by its slow weathering relative to other orthosilicates and coexisting Fe-silicates. Slow weathering of staurolite relative to most other silicate minerals may be due to the presence of stable kyanite-like "ribbons" in the staurolite structure or to the low site energy of the Fe-site in the staurolite structure (compared to other orthosilicates). Staurolite's slow weathering prevents the release of product-forming elements (especially Al) at rates sufficient to produce local supersaturation with respect to secondary minerals. Consequently, Al cannot behave conservatively on the scale of the dissolution site, and secondary minerals are not formed in sufficient proximity to the dissolution site to act as protective surface layers.

Protective surface layers can form in situations where Al is abundant; although this was not observed in any materials examined for this study, a few possible examples of protective-surface-layer-like textures are described in the literature from some bauxitic and lateritic weathering profiles. Protective surface layers of gibbsite may form in some bauxites, where Al can be derived both from the staurolite itself and, more importantly, by remobilization from the surrounding bauxitic matrix. It is well known that Al can be either depleted or enriched in different lateritic and bauxitic weathering horizons and landscape positions; depletion and enrichment take place simultaneously in different parts of the same profile or landscape, and the same volume of weathered material can experience multiple episodes of Al depletion and enrichment at different stages of its evolution (Boulangé, 1983, 1984, 1987; Nahon and Bocquier, 1983; Nahon, 1991; Delvigne, ms). An external source of abundant Al permits gibbsite saturation to be exceeded even in the vicinity of staurolite surfaces which are themselves weathering too slowly to favor conservative behavior of staurolite-derived Al. In these cases, staurolite weathering may be transport-limited.

#### ACKNOWLEDGMENTS

We thank the following for their contributions to this research: Salomon B. Kroonenberg, F. William Cambray, Alan Cressler, Thomas A. Vogel, and Allan B. Taylor, for providing samples and/or assistance

collecting samples; Jason R. Price for assistance with the SEM; Debra S. Bryan for assistance with sample preparation; Jill Banfield, Bruno Boulangé, Fabrice Colin, Jean Delvigne, Dennis Eberl, Steve Guggenheim, Daniel Nahon, and Sally J. Sutton for helpful and encouraging discussions; Kroonenberg, Colin, and Vogel for providing key references; Tina M. Beals for bibliographic assistance; and Danita S. Brandt for penetrating editorial scrutiny. The manuscript benefited from helpful reviews by an anonymous reviewer, the anonymous associate editor, and, especially, Lisa Stillings. This project was developed during a visit by the first author to the Laboratoire de Géosciences de l'Environnement, Université d'Aix-Marseille III; MAV is grateful to all his colleagues there for their hospitality. This research was supported by a grant from the Michigan State University Office of International Studies and Programs.

The first author dedicates this paper to the memory of his father, Anton Velbel.

## REFERENCES

- Bateman, R. M., and Catt, J. A., 1985, Modification of heavy mineral assemblages in English coversands by acid pedochemical weathering: *Catena*, v. 12, p. 1–21.
- Berner, R. A., 1978, Rate control of mineral dissolution under earth surface conditions: *American Journal of Science*, v. 278, p. 1235–1252.
- 1981, Kinetics of weathering and diagenesis, in Lasaga, A. C., and Kirkpatrick, R. J., editors, *Kinetics of Geochemical Processes*: Mineralogical Society of America, *Reviews in Mineralogy*, v. 8, p. 111–134.
- Berry, L. G., Mason, B., and Dietrich, R. V., 1983, *Mineralogy*, 2nd edition: San Francisco W. H. Freeman and Company, 561 p.
- Blackburn, W. H., and Dennen, W. H., 1994, *Principles of Mineralogy*, 2nd edition: Dubuque, Iowa, W. C. Brown Publishers, 413 p.
- Boulangé, B., 1983, Aluminium concentration in a bauxite derived of granite (Ivory Coast): Relative and absolute accumulations: *Travaux ICSOBA (International Committee for the Study of Bauxite and Aluminum)*, v. 13, p. 109–120.
- 1984, Les formations bauxitiques latéritiques de Côte-d'Ivoire: *Travaux et Documents de l'Orstom*, no. 175, 363 p.
- 1987, Relation between lateritic bauxitization and evolution of landscape: *Travaux ICSOBA (International Committee for the Study of Bauxite and Aluminum)*, v. 16–17, p. 155–162.
- Bryant, P. V., and Walther, J. V., 1992, Surface chemistry and silicate dissolution at elevated temperatures: *American Journal of Science*, v. 292, p. 639–658.
- Cambray, F. W., 1977, *The Geology of the Marquette District: A Field Guide*: East Lansing, Michigan, Basin Geological Society Guidebook, 62 p.
- Carmichael, D. M., Moore, J. M., Jr., and Skippen, G. B., 1978, Isograds around the Hastings metamorphic "low", in Currie, A. L., and Mackasey, W. O., editors, *Toronto '78: Field Trip Guidebook for the joint annual meeting of the Geological Society of America, the Geological Association of Canada, and the Mineralogical Association of Canada*, Toronto, 1978, p. 325–346.
- Casey, W. H., and Westrich, H. R., 1992, Control of dissolution rates of orthosilicate minerals by divalent metal-oxygen bonds: *Nature*, v. 355, p. 157–159.
- Deer, W. A., Howie, R. A., and Zussman, J., 1962, *Rock Forming Minerals*, v. 5, *Non-Silicates*: Longmans, 371 p.
- 1992, *An Introduction to the Rock-Forming Minerals*, 2nd edition: Longman Scientific & Technical, 696 p.
- Donnay, J. D. H., and Donnay, G., 1983, The staurolite story: *TMPM Tschermaks Mineralogische und Petrographische Mitteilungen*, v. 31, p. 1–15.
- Dowty, E., 1988, SHAPE: A computer program for drawing crystals.
- Dyar, M. D., Perry, C. L., Rebert C. R., Dutrow, B. L., Holdaway, M. J., and Lang, H. M., 1991, Mossbauer spectroscopy of synthetic and naturally occurring staurolite: *American Mineralogist*, v. 76, p. 27–41.

- Edou-Minko, A., ms, 1988, Petrologie et geochimie des laterites a "stone-line" du gite d'or d'Ovala—Application a la prospection en zone equatoriale humide (Gabon): Thesis, University of Poitiers, 147 p.
- Griffen, D. T., and Ribbe, P. H., 1973, The crystal chemistry of staurolite: *American Journal of Science*, v. 273-A, p. 479–495.
- Gupta, L. N., and Guha, D. B., 1985, Electron microscopic investigations of surface features in andalusite and staurolite: *The Indian Mineralogist*, v. 26, p. 23–26.
- Hatcher, R. D., Jr., 1979, The Coweeta Group and Coweeta syncline: Major features of the North Carolina-Georgia Blue Ridge: *Southeastern Geology*, v. 21, p. 17–29.
- 1980, Geologic Map and Mineral Resources Summary of the Prentiss Quadrangle, North Carolina, including Geologic Map of Coweeta Laboratory: North Carolina Department of Natural Resources and Community Development, Geological Survey Section, GM-167-SW and MRS 167-SW.
- 1988, Bedrock geology and regional setting of Coweeta Hydrologic Laboratory in the eastern Blue Ridge, in Swank, W. T., and Crossley, D. A., Jr., editors, *Forest Hydrology and Ecology at Coweeta*: New York, Springer Ecological Studies Series, no. 66, p. 81–92.
- Hawthorne, F. C., Ungaretti, L., Oberti, R., Caucia, F., and Callegari, A., 1993a, The crystal chemistry of staurolite. I. Crystal structure and site populations: *Canadian Mineralogist*, v. 31, p. 551–582.
- 1993b, The crystal chemistry of staurolite. II. Order-disorder and the monoclinic → orthorhombic phase transition: *Canadian Mineralogist*, v. 31, p. 583–595.
- 1993c, The crystal chemistry of staurolite. III. Local order and chemical composition: *Canadian Mineralogist*, v. 31, p. 597–616.
- Holdaway, M. J., Mukhopadhyay, B., Dyar, M. D., Dutrow, B. L., Rumble, D., III, and Grambling, J. A., 1991, A new perspective on staurolite crystal chemistry: Use of stoichiometric and chemical end-members for a mole fraction model: *American Mineralogist*, v. 76, p. 1910–1919.
- Hounslow, A. W., and Moore, J. M., Jr., 1967, Chemical petrology of Grenville schists near Fernleigh, Ontario: *Journal of Petrology*, v. 8, p. 1–28.
- James, H. L., 1955, Zones of regional metamorphism in the Precambrian of northern Michigan: *Geological Society of America Bulletin*, v. 66, p. 1455–1488.
- Lefebvre, A., 1982, Lattice defects in three structurally related minerals: Kyanite, yoderite and staurolite: *Physics and Chemistry of Minerals*, v. 8, p. 251–256.
- Morton, A. C., 1979, Surface features of heavy mineral grains from Paleocene sands of the central North Sea: *Scottish Journal of Geology*, v. 15, p. 293–300.
- 1984, Stability of detrital heavy minerals in Tertiary sandstones from the North Sea Basin: *Clay Minerals*, v. 19, p. 287–308.
- 1985, Heavy minerals in provenance studies, in Zuffa, G. G., editor, *Provenance of Arenites*: Dordrecht, D. Reidel, p. 249–277.
- Nahon, D. B., 1991, Introduction to the Petrology of Soils and Chemical Weathering: New York, John Wiley & Sons, Inc., 313 p.
- Nickel, E., 1973, Experimental dissolution of light and heavy minerals in comparison with weathering and intrastratal dissolution: *Contributions to Sedimentology*, v. 1, p. 1–68.
- Ribbe, P. H., 1982, Staurolite, in Ribbe, P. H., editor, *Orthosilicates* (second edition): Mineralogical Society of America, *Reviews in Mineralogy*, v. 5, p. 171–188.
- Schott, J. and Petit, J.-C., 1987, New evidence for the mechanisms of dissolution of silicate minerals, in Stumm, W., editor, *Aquatic Surface Chemistry: Chemical Processes at the Particle-Water Interface*: New York, John Wiley & Sons, Inc., p. 293–315.
- Smyth, J. R., and Bish, D. L., 1988, *Crystal Structures and Cation Sites of the Rock-Forming Minerals*: Boston, Allen & Unwin, 332 p.
- van Kersen, J. F., 1955, Bauxite deposits in Suriname and Demerara (British Guiana): *Leidse Geologische Mededelingen*, v. 21, p. 247–375.
- Velbel, M. A., 1984, Natural weathering mechanisms of almandine garnet: *Geology*, v. 12, p. 631–634.
- 1993, Formation of protective surface layers during silicate-mineral weathering under well-leached, oxidizing conditions: *American Mineralogist*, v. 78, p. 408–417.
- Welton, J. E., 1984, SEM Petrology Atlas: American Association of Petroleum Geologists, *Methods in Exploration Series*, 237 p.
- Westrich, H. R., Cygan, R. T., Casey, W. H., Zemitis, C., and Arnold, G. W., 1993, The dissolution kinetics of mixed-cation orthosilicate minerals: *American Journal of Science*, v. 293, p. 869–893.